# Ultrahigh thermal conductivity of isotopically enriched silicon

Alexander V. Inyushkin,[1,a)] Alexander N. Taldenkov,[1,b)] Joel W. Ager III,[2,3,c)] Eugene E. Haller,[2,3,d)] Helge Riemann,[4,e)] Nikolay V. Abrosimov,[4,f)] Hans-Joachim Pohl,[5,g)] and Peter Becker[6,h)]

[1]*National Research Center Kurchatov Institute, Moscow 123182, Russia*
[2]*Materials Sciences Division, Lawrence Berkeley National Laboratory, Berkeley, California 94720, USA*
[3]*Department of Materials Science and Engineering, University of California at Berkeley, Berkeley, California 94720, USA*
[4]*Leibniz-Institut für Kristallzüchtung, 12489 Berlin, Germany*
[5]*VITCON Projectconsult GmbH, 07745 Jena, Germany*
[6]*Physikalisch-Technische Bundesanstalt, Bundesallee 100, 38116 Braunschweig, Germany*

(Received 30 November 2017; accepted 10 February 2018; published online 6 March 2018)

Most of the stable elements have two and more stable isotopes. The physical properties of materials composed of such elements depend on the isotopic abundance to some extent. A remarkably strong isotope effect is observed in the phonon thermal conductivity, the principal mechanism of heat conduction in nonmetallic crystals. An isotopic disorder due to random distribution of the isotopes in the crystal lattice sites results in a rather strong phonon scattering and, consequently, in a reduction of thermal conductivity. In this paper, we present new results of accurate and precise measurements of thermal conductivity $\kappa(T)$ for silicon single crystals having three different isotopic compositions at temperatures $T$ from 2.4 to 420 K. The highly enriched crystal containing 99.995% of $^{28}$Si, which is one of the most perfect crystals ever synthesized, demonstrates a thermal conductivity of about $450 \pm 10$ W cm$^{-1}$K$^{-1}$ at 24 K, the highest measured value among bulk dielectrics, which is ten times greater than the one for its counterpart $^{nat}$Si with the natural isotopic constitution. For highly enriched crystal $^{28}$Si and crystal $^{nat}$Si, the measurements were performed for two orientations [001] and [011], a magnitude of the phonon focusing effect on thermal conductivity was determined accurately at low temperatures. The anisotropy of thermal conductivity disappears above 31 K. The influence of the boundary scattering on thermal conductivity persists sizable up to much higher temperatures (~80 K). The $\kappa(T)$ measured in this work gives the most accurate approximation of the intrinsic thermal conductivity of single crystal silicon which is determined solely by the anharmonic phonon processes and diffusive boundary scattering over a wide temperature range. *Published by AIP Publishing.*
https://doi.org/10.1063/1.5017778

## I. INTRODUCTION

In a number of semiconductor crystals with natural isotopic compositions of elements, the thermal resistivity due to isotope scattering of phonons adds sizably to the total resistivity at room temperature, and may dominate strongly over others at low temperatures (see, e.g., surveys in Refs. 1 and 2). Experimental studies showed that the isotope effect on thermal conductivity for crystals with natural isotopic abundances amounts to 50% for diamond,[3–6] 20% for germanium,[7–9] about 10% for silicon,[10–12] and 5% for GaAs[13] at room temperature. In chemically pure and defect-free crystals, the magnitude of the isotope effect depends on the rates of isotope scattering and anharmonic phonon-phonon scattering, the latter of which are intrinsic scattering processes governing thermal conductivity at high temperatures.

The phonon scattering induced by the isotopic disorder in the crystal lattice is a relatively simple phenomena, and its scattering rate can be calculated reliably in many cases, especially for the normal ("non-quantum") crystals.[14–16] For this reason, the experimental data on the isotope effect in thermal conductivity is used commonly to validate different theoretical models of heat conduction in crystals. They include various modifications of the Callaway theory[17] based on the Boltzmann transport equation and formulated within a single-mode relaxation time approximation,[5,9,17–20] and new *ab initio* Boltzmann transport approaches.[21–26] In theoretical calculations, the estimation of the phonon-phonon scattering processes is an especially challenging task (see, for example, Refs. 24 and 27–29). In this respect, experimental data on thermal conductivity of a single-isotope crystal are the most valuable since they represent almost solely the phonon-phonon processes over a wide temperature range.

The most accurate measurements of thermal conductivity for isotopically modified single crystal silicon have been performed in Refs. 10 and 12. The isotopic enrichment of the

[a)]Inyushkin_AV@nrcki.ru
[b)]Taldenkov_AN@nrcki.ru
[c)]jwager@lbl.gov
[d)]eehaller@lbl.gov
[e)]helge.riemann@ikz-berlin.de
[f)]nikolay.abrosimov@ikz-berlin.de
[g)]pohl.vitcon@t-online.de
[h)]peter.becker@ptb.de

crystal studied in Ref. 10 was low, 99.896% $^{28}$Si, and the temperature interval of measurements was restricted within 80–300 K. In Ref. 12 the enrichment was higher, 99.983% $^{28}$Si and $\kappa(T)$ was measured in a much wider temperature range from 0.5 to 300 K. The coincidence of the data for $^{28}$Si and $^{nat}$Si at low temperatures proved the consistency of the data obtained in that work.[12]

In this paper, we report on the thermal conductivity measurements of silicon single crystals with three different isotopic compositions and orientations including the most perfect nowadays single crystal silicon highly enriched up to 99.995% with the isotope $^{28}$Si. In this unique crystal, grown under the Avogadro project,[30] the isotopic scattering rate of phonon is reduced by 4 times as compared with that in the enriched crystal $^{28}$Si studied in Ref. 12 and by 2500 times lower than in the crystal with natural isotopic abundance. The prime goals of this work were the accurate and precise determination of the *intrinsic* thermal conductivity of silicon in a wide temperature range and the magnitude of the phonon focusing effect in thermal conductivity.

## II. MATERIALS AND METHODS

Single crystals of silicon with different isotopic composition were grown by the floating zone process in the Institute of Crystal Growth (IKZ, Berlin, Germany). The silicon boules were dislocation free. Concentrations of electrically active impurities P and B were approximately $5 \times 10^{15}$ cm$^{-3}$ and $2 \times 10^{14}$ cm$^{-3}$, respectively, and of carbon and interstitial oxygen were $<1 \times 10^{16}$ cm$^{-3}$ and $1.6 \times 10^{14}$ cm$^{-3}$, respectively, in the crystal $^{28}$SiB (see Ref. 31 for details). The crystal $^{28}$SiA was cut from the parent crystalline boule number Si28-10Pr11 grown within the Avogadro project in 2007.[30,32] It had the concentration of carbon of $<5 \times 10^{14}$ cm$^{-3}$, of oxygen of $<1 \times 10^{14}$ cm$^{-3}$, of all others impurities of $<1 \times 10^{14}$ cm$^{-3}$, and of vacancies of $\sim 3 \times 10^{14}$ cm$^{-3}$.[33] The isotopic parameters of these crystals are listed in Table I. The dimensionless parameter

$$g_2 = \sum_i f_i (\Delta M_i / M)^2 \tag{1}$$

characterizes the isotopic disorder. Here, $f_i$ is the concentration of the $i$-th isotope, whose mass $M_i$ differs from the average mass $M = \sum_i f_i M_i$ by $\Delta M_i = M_i - M$.

The impurity concentrations indicated above are the upper bounds for them; according to electrical measurements, the concentration of electrically active impurities might be an order of magnitude lower in the samples fabricated for thermal conductivity measurements. The phonon scattering rate from single impurity atoms is proportional to[34]

$$g_2^{(\mathrm{imp})} = \sum_j f_j \left(\Delta M_j / M + 2\gamma\alpha\right)^2, \tag{2}$$

where $\Delta M_j$ is the mass defect of the impurity $j$, $M$ is the host atom mass, $\gamma$ is the Grüneisen constant ($\sim$1 for silicon), and $\alpha$ is the fractional volume difference between impurity and host atoms. The values of $\alpha$ were estimated from the data presented in Ref. 33. We estimated that carbon (with $g_2^{(\mathrm{C})} < 7 \times 10^{-8}$) and vacancies ($g_2^{(\mathrm{vac})} < 3 \times 10^{-8}$) might be dominant scatterers in the samples $^{28}$SiA. In the case of samples $^{28}$SiB, the majority contributors might be phosphorus ($g_2^{(\mathrm{P})} < 2.5 \times 10^{-6}$), boron ($g_2^{(\mathrm{B})} < 1.4 \times 10^{-6}$), and carbon ($g_2^{(\mathrm{C})} < 1.3 \times 10^{-6}$). It is seen that at most the total $g_2^{(\mathrm{imp})}$ value for impurities is similar to the isotopic $g_2$ value in isotopically enriched crystals. This is the estimation from above since the concentrations of impurities are at and below the detection limits. For crystals with natural isotopic composition, the effect impurities are negligible as compared with the isotopes.

Rectangular silicon rods were cut from the ingots using a diamond saw. These rods had approximately 4.35 $\times$ 4.35 mm$^2$ cross-section and a length of about 40 mm. The rods were subjected to hand lapping with an abrasive powder suspended in water. The powder grit size of 40 $\mu$m was used to lap all rod surfaces to a side dimension of 4.10 mm. The final lapping was performed with 14 $\mu$m grit abrasive powder. The average surface roughness amplitude $R_a$ was measured to be 0.20–0.25 $\mu$m. Note that the sub-surface damage layer with the strongly modified properties of silicon is estimated to be about as thick as the abrasive grit size used.[35] The final side dimensions of the samples were 4.00 $\pm$ 0.005 mm. The isotopic composition, orientation, and dimensions of the samples are given in Table II.

Thermal conductivity was measured from 2.4 to 420 K by the steady-state heat flow technique with two thermometers and one heater. A thick film resistor with 6.3 $\times$ 3.2 $\times$ 0.55 mm$^3$ dimensions and room temperature resistance of 365 $\Omega$ was used as a gradient heater. It was glued to a sample end with a silver-filled epoxy. The resistive thermometers Cernox CX-1050-SD (Lake Shore Cryotronics, Inc.) were

TABLE I. Characteristics of crystals. $\Delta N = |N_d - N_a|$ is the net concentration of the electrically active impurities as estimated from the electrical resistivity at room temperature.

| Crystal | $^{28}$Si % | $^{29}$Si % | $^{30}$Si % | $g_2$ $10^{-6}$ | Type | $\rho$ $\Omega$ cm | $\Delta N$ $10^{12}$ cm$^{-3}$ |
|---|---|---|---|---|---|---|---|
| $^{nat}$SiA | 92.223 | 4.685 | 3.092 | 200.7 | *p* | 2340 | 5.5 |
| $^{nat}$SiB | 92.223 | 4.685 | 3.092 | 200.7 | *n* | 1010 | 4.3 |
| $^{28}$SiA | 99.995 | 0.0046 | 0.0004 | 0.08 | *p* | 1020 | 13 |
| $^{28}$SiB | 99.92 | 0.075 | 0.005 | 1.21 | *n* | 7.4 | 600 |

TABLE II. Sample characteristics. $L$ is the total sample length and $L_T$ is the distance between two thermometers attached to a sample. Absolute error is 0.1 mm in the sample length, the value of $L_T$ is known within 0.2–0.3 mm uncertainty.

| Sample | $^{28}$Si % | Axis | $L$ mm | $L_T$ mm | $T_{max}$ K | $\kappa_{max}$ W cm$^{-1}$ K$^{-1}$ |
|---|---|---|---|---|---|---|
| $^{nat}$SiA100 | 92.223 | [100] | 40.0 | 27.3 | 22.3 | 45.5 |
| $^{nat}$SiA110 | 92.223 | [110] | 40.0 | 28.2 | 23.9 | 43.8 |
| $^{nat}$SiB100 | 92.223 | [100] | 39.5 | 26.8 | 22.3 | 45.7 |
| $^{28}$SiA100 | 99.995 | [100] | 38.5 | 26.7 | 24.1 | 450 |
| $^{28}$SiA110 | 99.995 | [110] | 40.2 | 26.3 | 25.3 | 420 |
| $^{28}$SiB100 | 99.92 | [100] | 39.5 | 27.7 | 24.5 | 280 |

used for the temperature measurements. The thermometers were calibrated in the International Temperature Scale of 1990 (ITS-90). Indium-faces copper clamps were used to attach the thermometers to a sample. The widths of contacts were 0.5–0.6 mm; the distance between two thermometers $L_T$, more correctly called as a mean separation between thermometer clamps, was about 27 mm (see Table II). The thermal length $L_{th}$, that is the length over which the temperature gradient was established in a sample, was approximately 4 mm smaller than the total length $L$.

Under steady conditions, the temperature difference $\Delta T$ between thermometers was controlled to be small, 0.002–0.8 K. In order to reduce the systematic error in measurements of $\Delta T$, the two stage procedure was employed: with gradient heater (1) off and (2) on. The temperature controller maintained the temperature at the position of the cold thermometer is constant on both steps. The $\Delta T$ was determined as a difference between values of the second "hot" thermometer on the heater on and off.[36] The random errors in $\Delta T$ were reduced by averaging over a large number of readings, >200, from thermometers. By this, the sensitivity up to 40 $\mu$K (near 24 K) was achieved. A multi-layer radiation shield was mounted around the sample in order to reduce radiation heat losses from the heater and sample at temperatures above 300 K. Small corrections to measured data at these temperatures, which take into account the effect of remanent (residual) heat loses were applied. The uncertainty in the absolute value of thermal conductivity is estimated to be less than 2% over almost all temperature intervals measured. The uncertainty in the determination of thermometer separation contributes substantially to this error. At high temperatures, above approximately 300 K, an experimental error due to radiation heat loses increases very rapidly with temperature. We estimate that this experimental error is $\lesssim$2% at 420 K.

## III. RESULTS AND DISCUSSION

Experimental data on the temperature dependence of thermal conductivity of natural and enriched silicon crystals with the [100] rod axis are shown in Fig. 1. The thermal conductivity for three samples of $^{nat}$Si has been measured. Two of them originate from the same parent crystal $^{nat}$SiA (see Table I), and have different orientations. All samples of $^{nat}$Si exhibit very similar $\kappa(T)$ dependence in the overall temperature range studied. In Fig. 2, the comparison of our experimental data for silicon of natural isotopic composition with the reference data $\kappa_{ref}(T)$ from Ref. 37 is shown. At low temperatures, where the $\kappa(T)$ depends on the sample dimensions, the comparison is meaningless. At high temperatures, above 80 K, there is an overall good agreement between the data. However, the deviation, $\kappa(T)/\kappa_{ref}(T) - 1$, shows anomaly at 150 K. Since our highly accurate and precise data demonstrate quite smooth dependencies $\kappa(T)$, it appears that the reference data have a systematic error reaching 4% within the temperature interval $120 < T < 300$ K.

The maximum value of thermal conductivity over all samples is obtained for the most pure sample $^{28}$SiA100. It equals to 450±10 W cm$^{-1}$K$^{-1}$ at 24.1 K. This value is the highest ever measured till now value for thermal conductivity of dielectrics at any temperature. The previous record, $\kappa = 410$ W cm$^{-1}$K$^{-1}$ at 104 K, was set for the isotopically pure single crystal diamond $^{12}$C(99.9%).[5]

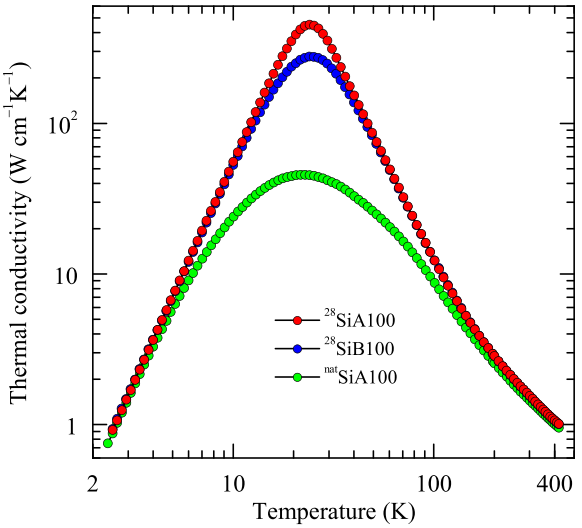


FIG. 1. Thermal conductivity of silicon single crystals along the [100] axis as a function of temperature. Data for three crystals with different isotopic compositions are shown.

All enriched crystals show a symmetric, single, and sharp peak in $\kappa(T)$ at low temperatures (see Fig. 1). This peak shape is rather contrasting with the calculated dependencies $\kappa(T)$, which were obtained using generalized Callaway models that rely on the assumption that phonons of different polarizations independently contribute to the total conductivity.[19,20] These calculated $\kappa(T)$ demonstrate asymmetric and broad peaks arising from a large difference of the phonon velocities for different polarizations. A similar result was obtained for germanium in Refs. 9 and 19.

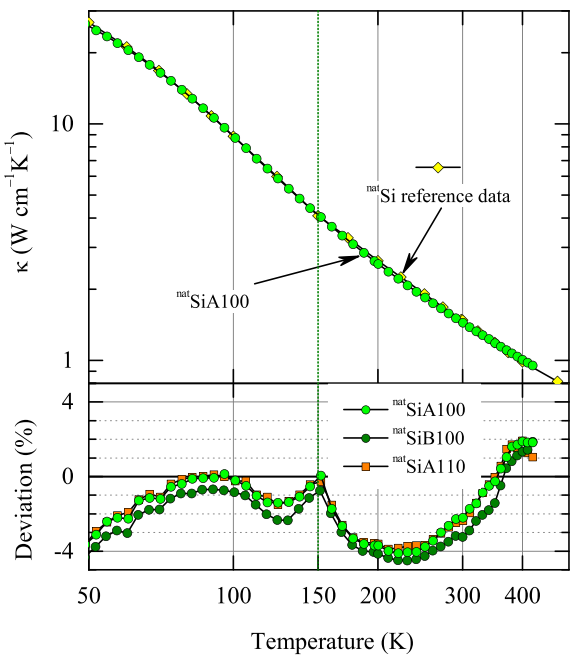


FIG. 2. Thermal conductivity as a function of temperature for silicon samples of natural isotopic composition. The lower panel: the relative difference between our data and the reference one.[37]

In Fig. 3, the ratio of thermal conductivities of enriched crystals to that of $^{nat}$SiB100 as a function of temperature is shown. At the maximum, the ratio attains 10 and the temperature of the maximum is about 24 K. The isotope effect (for the crystal with natural isotopic abundance) becomes almost zero at $T < 2.5$ K. On the other hand, the effect decreases at high temperatures being about $8 \pm 1\%$ at 298 K (see the inset in Fig. 3). This value is close to that (7%–10%) found in Refs. 10–12. At liquid nitrogen temperature (78 K), the isotope effect accounts 75%. From Figs. 1 and 3, it is seen that dependencies $\kappa(T)$ for $^{28}$SiA and $^{28}$SiB are the same within experimental errors at $60 < T < 420$ K. This suggests that the thermal conductivity of silicon does not depend upon the isotopic composition at the concentration of isotope $^{28}$Si above 99.92% in this temperature range. That is, the isotope scattering is much weaker than the phonon-phonon scattering. Below 60 K, the isotope scattering contribution to the thermal conductivity in sample $^{28}$SiB increases sizably with decreasing temperature. At 40 K, the thermal resistivity of $^{28}$SiB is about 12% higher than that of $^{28}$SiA due to this scattering. Since the isotope scattering rate for $^{28}$SiB is 15 times the rate for $^{28}$SiA (see $g_2$ values in Table I), this scattering appears to be unimportant in the thermal conductivity of $^{28}$SiA above about 40 K.

The $\kappa(T)$ for the enriched crystals is very close to the cubic dependence at temperatures below 10 K that is expected for the regime of purely diffusive boundary scattering of phonons. Specifically, we find that $\kappa(T) \propto T^n$, where $n = 2.97 \pm 0.06$ for the purest sample $^{28}$SiA. The exponent $n$ for $^{nat}$Si becomes equal to that for $^{28}$SiA below 2.5 K. Since the specific heat of the silicon crystal follows the cubic temperature dependence below 9 K,[38,39] our low temperature data on $\kappa(T)$ for the sample $^{28}$SiA suggest that the phonon mean free path reaches the maximum value determined only by the sample geometry and its orientation.

In Fig. 4, the dependencies of $\kappa(T)$ for two pairs of samples with different orientations are shown. These data demonstrate the effect of phonon focusing on the thermal

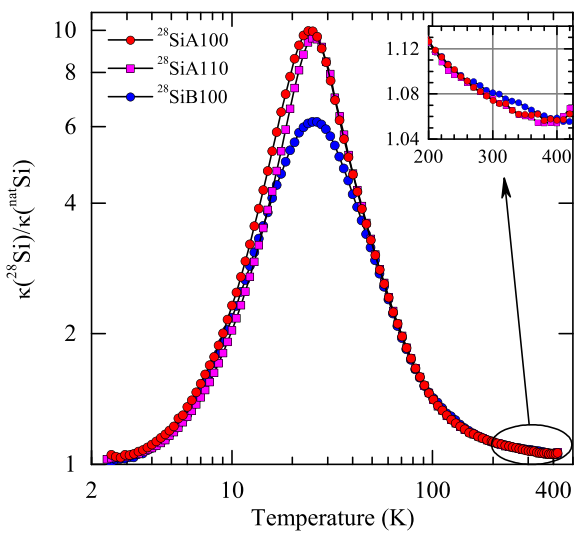


FIG. 3. The ratio of thermal conductivities of enriched crystals to that of $^{nat}$SiB100 as a function of temperature.

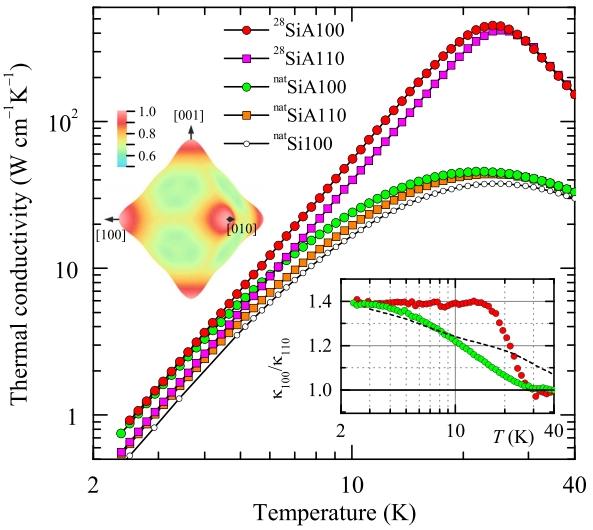


FIG. 4. The temperature dependencies of thermal conductivity for two pairs of samples with different orientations and isotopic compositions. The open circles denote the data from Ref. 12 for $^{nat}$Si oriented along [100] with a small cross-section $2.00 \times 3.12$ mm$^2$. The ratio of $\kappa[100]/\kappa[110]$ as a function of temperature is shown in the right-hand inset; the dash line is calculated from the data of Ref. 43. The left-hand inset shows the calculated orientation dependence of $\kappa$ at 3 K, the data normalized to 1 for the [100] direction.

conductivity of silicon. At temperatures near and below the thermal conductivity maximum, the $\kappa(T)$ for samples with [100] orientations is higher than that for [110] samples. The phonon focusing effect is clearly seen for isotopically enriched silicon. This effect becomes sizable at $T < 31$ K and the ratio $\kappa[100]/\kappa[110]$ stays nearly constant at 1.39 for temperatures below 14 K (the right-hand inset in Fig. 4). For $^{nat}$Si, the phonon focusing is also observed below 31 K, the ratio $\kappa[100]/\kappa[110]$ increases with decrease of temperature down to ≈3.5 K; this ratio is about 1.38 at 3 K and smaller than the value 1.43 measured in Ref. 40. According to the theory,[41] the ratio $\kappa[100]/\kappa[110] = 1.38$ for the silicon samples with the square cross section and $D/L = 0.1$, and our values equal this estimation within the experimental uncertainty. Note that, at temperature above which the phonon focusing effect begins to suppress with temperature, the phonon free path in the isotope scattering gets smaller than that in the boundary scattering for phonons with energy $3.8\ k_BT$ that dominate in thermal conduction. The 3D-plot of thermal conductivity for the silicon rod with the square cross-section as a function of orientation at 3 K in the boundary scattering regime is presented in Fig. 4, left-hand inset. These data were calculated using the theoretical approach developed in Ref. 42. Above 31 K, the conductivity is isotropic, as it must be for cubic crystals.

We estimated the phonon free path $l_b$ in the boundary scattering for samples $^{28}$SiA100 using the well known expression (see, for example, Ref. 40)

$$\kappa = \frac{1}{3} C_v\, v_C\, l_b, \tag{3}$$

where $C_v$ is the specific heat per unit volume and $v_C$ is the Casimir sound velocity ($5.66 \times 10^5$ cm/s for silicon[40]). From

our experimental $\kappa(T)$ data and specific heat data[38,39] for $T < 9$ K, we have found that $l_b = 4.96$ and 3.57 mm for 28SiA100 and 28SiA110, respectively. The theoretical Casimir length $l_C$ (corrected for the finite sample length) for our samples is 3.72 mm. So the phonon free path reaches the cross-sectional dimension; the ratio $l_b/l_C = 1.33$ and 0.96 for [100] and [110] directions, respectively, in full accord with the theoretical results of McCurdy.[40,41]

In Fig. 4, the experimental $\kappa(T)$ for the $^{nat}$Si rod with smaller cross-section and orientation [100] is shown ($^{nat}$Si100, Ref. 12). As expected, it lies below the curve of its larger counterpart $^{nat}$SiA100 due to the higher rate of phonon boundary scattering in $^{nat}$Si100. The conductivity of $^{nat}$Si100 is lower sizably than that of the larger rod even at temperatures up to 80–100 K, much higher than 31 K, at which the focusing effect dies out. It appears that the prerequisite of the phonon focusing effect in thermal conductivity is the long phonon mean free path comparable or exceeding the cross-section dimensions of a sample, and the absence of phonon-phonon interactions. The calculations of $\kappa(T)$ within the Callaway theory in Ref. 43 did not reproduce such steep decreasing of the phonon focusing effect with temperature increase in silicon (the dash line in Fig. 4, right-hand inset).

## IV. CONCLUSIONS

In summary, the thermal conductivity of three crystals of silicon with different isotopic composition has been measured accurately from 2.4 to 420 K. The isotope effect is $8 \pm 1\%$ for silicon with natural isotopic composition at room temperature. The thermal conductivity of a single isotope crystal containing 99.995% of $^{28}$Si reaches the maximum of 450 W cm$^{-1}$K$^{-1}$ at 24 K, the highest value measured for dielectrics till now. This crystal shows nearly exact $T^3$ dependence of $\kappa(T)$ at temperatures below approximately 10 K. At temperatures below 31 K, the thermal conductivity of the silicon rod with orientation [100] is higher than that of the rod with orientation [110] due to the phonon focusing effect.

From the precise data obtained in this work, it appears that the reference data values on $\kappa(T)$ for single crystal silicon with natural isotopic composition near 150 K are inconsistent with the rest of the data within about 4% below 300 K. Our measured $\kappa(T)$ for highly enriched silicon $^{28}$Si provides the most accurate approximation of the true temperature dependence of thermal conductivity of silicon governed solely by the intrinsic phonon-phonon scattering processes at temperatures from near the conductivity maximum to 420 K. The experimental data of this work, including the dependencies on the isotope concentration and crystal orientation, provide a solid base for the verification of modern quantitative theories for the heat transport in dielectrics.

## ACKNOWLEDGMENTS

The work was partially supported by the NRC "Kurchatov Institute," Russian Foundation for Basic Research through Grant No. 16-07-00979. J.W.A. and E.E.H. were supported by the Electronic Materials program, funded by the Director, Office of Science, Office of Basic Energy Sciences, Materials Sciences and Engineering Division of the U.S. Department of Energy under Contract No. DE-AC02-05CH11231. The enriched samples 28SiA used in this study were prepared from Avo28 material produced by the International Avogadro Coordination (IAC) Project (2004–2011) in cooperation among the BIPM, the IN-RIM (Italy), the IRMM (EU), the NMIA (Australia), the NMIJ (Japan), the NPL (UK), and the PTB (Germany). The authors thank Professor I. G. Keleyev, Dr. I. I. Kuleyev, and Dr. A. M. Gibin for the helpful discussion.

[1]E. E. Haller, J. Appl. Phys. **77**, 2857 (1995).
[2]A. P. Zhernov and A. V. Inyushkin, Phys.-Usp. **45**, 527 (2002).
[3]T. R. Anthony, W. F. Banholzer, J. F. Fleischer, L. Wei, P. K. Kuo, R. L. Thomas, and R. W. Pryor, Phys. Rev. B **42**, 1104 (1990).
[4]J. R. Olson, R. O. Pohl, J. W. Vandersande, A. Zoltan, T. R. Anthony, and W. F. Banholzer, Phys. Rev. B **47**, 14850 (1993).
[5]L. Wei, P. K. Kuo, R. L. Thomas, T. R. Anthony, and W. F. Banholzer, Phys. Rev. Lett. **70**, 3764 (1993).
[6]A. A. Kaminskii, V. G. Ralchenko, H. Yoneda, A. P. Bolshakov, and A. V. Inyushkin, JETP Lett. **104**, 347 (2016) [Pis'ma Zh. Eksp. Teor. Fiz. **104**, 356 (2016) (in Russian)].
[7]T. H. Geballe and G. W. Hull, Phys. Rev. **110**, 773 (1958).
[8]V. I. Ozhogin, A. V. Inyushkin, A. N. Taldenkov, A. V. Tikhomirov, G. E. Popov, E. Haller, and K. Itoh, JETP Lett. **63**, 490 (1996) [Pis'ma Zh. Eksp. Teor. Fiz. **63**, 463 (1996)].
[9]M. Asen-Palmer, K. Bartkowski, E. Gmelin, M. Cardona, A. P. Zhernov, A. V. Inyushkin, A. N. Taldenkov, V. I. Ozhogin, K. M. Itoh, and E. E. Haller, Phys. Rev. B **56**, 9431 (1997).
[10]A. V. Gusev, A. M. Gibin, O. N. Morozkin, V. A. Gavva, and A. V. Mitin, Inorg. Mater. **38**, 1100 (2002) [Neorg. Mater. **38**, 1305 (2002) (in Russian)].
[11]R. K. Kremer, K. Graf, M. Cardona, G. G. Devyatykh, A. V. Gusev, A. M. Gibin, A. V. Inyushkin, A. N. Taldenkov, and H.-J. Pohl, Solid State Commun. **131**, 499 (2004).
[12]A. V. Inyushkin, A. N. Taldenkov, A. M. Gibin, A. V. Gusev, and H.-J. Pohl, Phys. Status Solidi C **1**, 2995 (2004).
[13]A. V. Inyushkin, A. N. Taldenkov, A. Yu. Yakubovsky, A. V. Markov, L. Moreno-Garsia, and B. N. Sharonov, Semicond. Sci. Technol. **18**, 685 (2003).
[14]P. G. Klemens, Proc. Phys. Soc., London, Sec. A **68**, 1113 (1955).
[15]P. Carruthers, Rev. Mod. Phys. **33**, 92 (1961).
[16]S. Tamura, Phys. Rev. B **27**, 858 (1983).
[17]J. Callaway, Phys. Rev. **113**, 1046 (1959).
[18]R. Berman and J. C. F. Brock, Proc. R. Soc. London, Ser. A **289**, 46 (1965).
[19]D. T. Morelli, J. P. Heremans, and G. A. Slack, Phys. Rev. B **66**, 195304 (2002).
[20]I. G. Kuleev and I. I. Kuleev, J. Exp. Theor. Phys. **95**, 480 (2002) [Zh. Eksp. Teor. Fiz. **122**, 558 (2002) (in Russian)].
[21]M. Omini and A. Sparavigna, Nuovo Cimento D **19**, 1537 (1997).
[22]D. A. Broido, A. Ward, and N. Mingo, Phys. Rev. B **72**, 014308 (2005).
[23]D. A. Broido, M. Malorny, G. Birner, N. Mingo, and D. A. Stewart, Appl. Phys. Lett. **91**, 231922 (2007).
[24]A. Ward, D. A. Broido, D. A. Stewart, and G. Deinzer, Phys. Rev. B **80**, 125203 (2009).
[25]C. de Tomas, A. Cantarero, A. F. Lopeandia, and F. X. Alvarez, J. Appl. Phys. **115**, 164314 (2014).
[26]A. Jain and A. J. H. McGaughey, Comput. Mater. Sci. **110**, 115 (2015).
[27]I. G. Kuleyev, I. I. Kuleyev, and I. Yu. Arapova, J. Phys.: Condens. Matter **20**, 465201 (2008).
[28]K. Esfarjani, G. Chen, and H. T. Stokes, Phys. Rev. B **84**, 085204 (2011).
[29]J. Ma, W. Li, and X. Luo, Phys. Rev. B **90**, 035203 (2014).
[30]P. Becker, H.-J. Pohl, H. Riemann, and N. Abrosimov, Phys. Status Solidi A **207**, 49 (2010).
[31]J. W. Ager III, J. W. Beeman, W. L. Hansen, E. E. Haller, I. D. Sharp, C. Liao, A. Yang, M. L. W. Thewalt, and H. Riemann, J. Electrochem. Soc. **152**, G448 (2005).
[32]N. V. Abrosimov, D. G. Arefev, P. Becker, H. Bettin, A. D. Bulanov, M. F. Churbanov, S. V. Filimonov, V. A. Gavva, O. N. Godisov, A. V. Gusev,

T. V. Kotereva, D. Nietzold, M. Peters, A. M. Potapov, H.-J. Pohl, A. Pramann, H. Riemann, P.-T. Scheel, R. Stosch, S. Wundrack, and S. Zakel, Metrologia **54**, 599 (2017).
[33]B. Andreas, Y. Azuma, G. Bartl, P. Becker, H. Bettin, M. Borys, I. Busch, M. Gray, P. Fuchs, K. Fujii, H. Fujimoto, E. Kessler, M. Krumrey, U. Kuetgens, N. Kuramoto, G. Mana, P. Manson, E. Massa, S. Mizushima, A. Nicolaus, A. Picard, A. Pramann, O. Rienitz, D. Schiel, S. Valkiers, and A. Waseda, Phys. Rev. Lett. **106**, 030801 (2011).
[34]L. A. Turk and P. G. Klemens, Phys. Rev. B **9**, 4422 (1974).
[35]H. Lundt, M. Kerstan, A. Huber, and P. O. Hahn, in *Proceedings of 7th International Symposium on Silicon Materials Science and Technology* (The Electrochemical Society, Pennington, NJ, 1994), Vols. 94–10, pp. 218–224.
[36]R. L. Cappelletti and M. Ishikawa, Rev. Sci. Instrum. **44**, 301 (1973).
[37]C. Y. Ho, R. W. Powell, and P. E. Liley, J. Phys. Chem. Ref. Data **1**, 279 (1972).
[38]P. Flubacher, A. J. Leadbetter, and J. A. Morrison, Philos. Mag. **4**, 273 (1959).
[39]A. Gibin, G. G. Devyatykh, A. V. Gusev, R. K. Kremer, M. Cardona, and H.-J. Pohl, Solid State Commun. **133**, 569 (2005).
[40]A. K. McCurdy, H. J. Maris, and C. Elbaum, Phys. Rev. B **2**, 4077 (1970).
[41]A. K. McCurdy, Phys. Rev. B **26**, 6971 (1982).
[42]I. I. Kuleev, I. G. Kuleev, S. M. Bakharev, and A. V. Inyushkin, Physica B **416**, 81 (2013).
[43]I. I. Kuleev, I. G. Kuleev, S. M. Bakharev, and A. V. Inyushkin, Phys. Status Solidi B **251**, 991 (2014).